Article
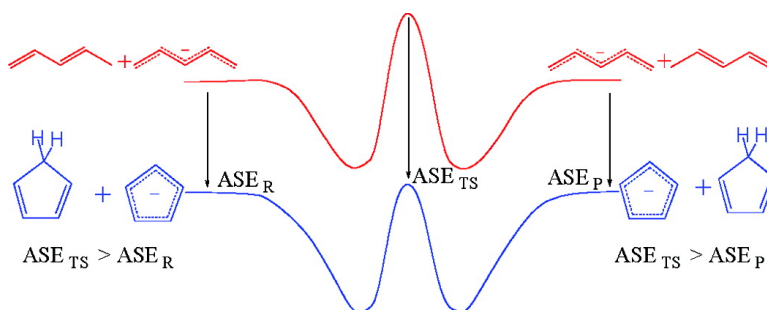
Proton Transfers in Aromatic and Antiaromatic Systems. How Aromatic or Antiaromatic Is the Transition State? An Ab Initio Study

Claude F. Bernasconi, Philip J. Wenzel, and Mark L. Ragains

More About This Article

Additional resources and features associated with this article are available within the HTML version:

- Supporting Information
- Links to the 2 articles that cite this article, as of the time of this article download
- Access to high resolution figures
- Links to articles and content related to this article
- Copyright permission to reproduce figures and/or text from this article

View the Full Text HTML

Proton Transfers in Aromatic and Antiaromatic Systems. How Aromatic or Antiaromatic Is the Transition State? An Ab Initio Study

Claude F. Bernasconi,* Philip J. Wenzel, and Mark L. Ragains

*Department of Chemistry and Biochemistry, University of California, Santa Cruz, California 95064*

Received October 25, 2007; E-mail: bernasconi@chemistry.ucsc.edu

Abstract: An ab initio study of six carbon-to-carbon identity proton transfers is reported. They refer to the benzenium ion/benzene ($C_6H_7^+$/C_6H_6), the 2,4-cyclopentadiene/cyclopentadienyl anion (C_5H_6/$C_5H_5^-$), and the cyclobutenyl cation/cyclobutadiene ($C_4H_5^+$/C_4H_4) systems and their respective noncyclic reference systems, that is, ⌇⌇/⌇⌇, ⌇⌇/⌇⌇ and ⌇⌇/⌇⌇. For the aromatic $C_6H_7^+$/C_6H_6 and C_5H_6/$C_5H_5^-$ systems, geometric parameters and aromaticity indices indicate that the transition states are highly aromatic. The proton-transfer barriers in these systems are quite low, which is consistent with a disproportionately high degree of transition-state aromaticity. For the anti-aromatic $C_4H_5^+$/C_4H_4 system, the geometric parameters and aromaticity indices indicate a rather small degree of antiaromaticity of the transition state. However, the proton-transfer barrier is higher than expected for a transition state with a low antiaromaticity. This implies that another factor contributes to the barrier; it is suggested that this factor is angle and torsional strain in the transition state. The question whether charge delocalization at the transition state might correlate with the development of aromaticity was also examined. No such correlation was found, that is, charge delocalization lags behind proton transfer as is commonly observed in nonaromatic systems involving π-acceptor groups.

Introduction

The concept of the intrinsic barrier or intrinsic rate constant of a reaction[1] is of central importance in dealing with chemical reactivity. This is because it allows one to separate the thermodynamic driving force on reaction barriers from purely kinetic effects. Hence, a deeper understanding of chemical reactivity depends very much on an understanding of the factors that affect intrinsic barriers.

Ideally, one would always want to determine intrinsic barriers or intrinsic rate constants when dealing with reactivity. However, this requires the determination of rate *and* equilibrium constants, which is not always possible or practical. One class of reactions that often *does* allow such measurements are proton transfers from carbon acids activated by π acceptors, as in eq 1. These

$$B^v + H-\overset{|}{\underset{|}{C}}-Y \longrightarrow BH^{v+1} + >C=Y^- \qquad (1)$$
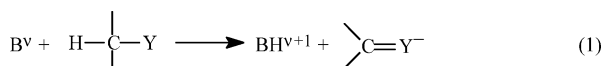
reactions are not only of great interest because of their ubiquity and fundamental nature, they can also serve as models for most polar rea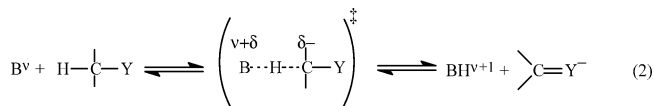ctions because they include all of the important features of such reactions, for example, bond changes, charge transfer, charge delocalization/resonance, steric, and solvation/desolvation effects.

Research from various laboratories, including our own, has demonstrated that the π-acceptor strength of the Y group has a dominant effect on the intrinsic barriers of these proton transfers, at least in solution, that is, the stronger the π acceptor the higher the intrinsic barrier.[4–8] This π-acceptor effect is the result of a transition-state imbalance, whereby the charge delocalization into the π acceptor of the carbanion lags behind proton transfer, as shown in an exaggerated

(1) The intrinsic barrier of a reaction with a forward rate constant k_1 and a reverse rate constant k_{-1} is defined as $\Delta G_0^\ddagger = \Delta G_1^\ddagger = \Delta G_{-1}^\ddagger$ when $\Delta G° = 0$; similarly, the intrinsic rate constant is defined as $k_0 = k_1 = k_{-1}$ when $K_1 = 1$.[2,3]
(2) Marcus, R. A. *J. Phys. Chem.* **1968**, *72*, 891.
(3) Keeffe, J. R.; Kresge, A. J. In *Investigation of Rates and Mechanisms of Reactions*; Bernasconi, C. F., Ed.; Wiley-Interscience: New York, 1986; Part 1, p 747.

(4) (a) Bernasconi, C. F. *Acc. Chem. Res.* **1987**, *20*, 301. (b) Bernasconi, C. F. *Acc. Chem. Res.* **1992**, *25*, 9. (c) Bernasconi, C. F. *Adv. Phys. Org. Chem.* **1992**, *27*, 119.
(5) (a) Bernasconi, C. F.; Sun, W.; García-Río, L.; Kin-Yan; Kittredge, K. *J. Am. Chem. Soc.* **1997**, *119*, 5583. (b) Bernasconi, C. F.; Ali, M. *J. Am. Chem. Soc.* **1999**, *121*, 3039. (c) Bernasconi, C. F.; Sun, W. *J. Am. Chem. Soc.* **2002**, *124*, 2799. (d) Bernasconi, C. F.; Ali, M.; Gunter, J. C. *J. Am. Chem. Soc.* **2003**, *125*, 151. (e) Bernasconi, C. F.; Fairchild, D. E.; Montañez, R. L.; Aleshi, P.; Zheng, H.; Lorance, E. *J. Org. Chem.* **2005**, *70*, 7721. (f) Bernasconi, C. F.; Ragains, M. L. *J. Organomet. Chem.* **2005**, *690*, 5616.
(6) (a) Terrier, F.; Lelièvre, J.; Chatrousse, A.-P.; Farrell, P. *J. Chem. Soc., Perkin Trans. 2* **1985**, 1479. (b) Terrier, F.; Xie, H.-Q.; Lelièvre, J.; Boubaker, T.; Farrell, P. G. *J. Chem. Soc., Perkin Trans. 2* **1990**, 1899. (c) Moutiers, G.; El Fahid, B.; Collet, A.-G.; Terrier, F. *J. Chem. Soc., Perkin Trans. 2* **1996**, 49. (d) Moutiers, G.; El Fahid, B.; Goumont, R.; Chatrousse, A.-P.; Terrier, F. *J. Org. Chem.* **1996**, *61*, 1978.
(7) (a) Nevy, J. B.; Hawkinson, D. C.; Blotny, G.; Yao, X.; Pollack, R. M. *J. Am. Chem. Soc.* **1997**, *119*, 12722. (b) Yao, X.; Gold, M.; Pollack. R. M. *J. Am. Chem. Soc.* **1999**, *121*, 6220.
(8) Zhong, Z.; Snowden, T. S.; Best, M. D.; Anslyn, E. V. *J. Am. Chem. Soc.* **2004**, *126*, 3488.
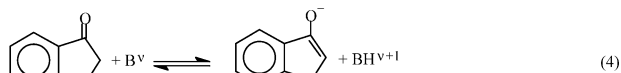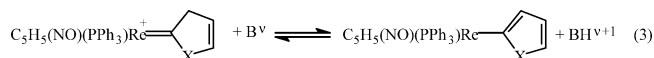(9) Kresge, A. J. *Can. J. Chem.* **1974**, *52*, 1897.

form in eq 2[4,9] (for a more nuanced representation see below). Because of this lag,

$$B^{\nu} + H-\overset{|}{\underset{|}{C}}-Y \rightleftharpoons \left(\overset{\nu+\delta}{B}\cdots H\cdots \overset{\delta-}{\underset{|}{C}}-Y \right)^{\ddagger} \rightleftharpoons BH^{\nu+1} + \,\,\diagup C=Y^{-} \quad (2)$$

the transition state derives only a minimal benefit from the stabilizing effect of charge delocalization, and this is the reason why the intrinsic barrier is high.[4] The same barrier enhancement occurs in the reverse direction because most of the resonance stabilization of the anion is lost at the transition state.[10]

The increase in the intrinsic barrier due to the transition-state imbalance is a manifestation of the principle of nonperfect synchronization (PNS);[4] it not only applies to resonance effects but to any product or reactant stabilizing factor (e.g., solvation, electrostatic effects, steric effects, polarizability effects, etc.) in any chemical reaction. The PNS states that a product stabilizing factor that lags behind bond changes at the transition state increases the intrinsic barrier, whereas a product-stabilizing factor that develops ahead of bond changes lowers the intrinsic barrier.[17] *This principle is mathematically provable and hence there can be no exception.*[4c]

Recently, we posed the question of whether the effect of product aromaticity on intrinsic barriers of proton transfers is qualitatively the same as the effect of resonance/charge delocalization, that is, does the development of aromaticity at the transition state also lag behind proton transfer, thereby increasing the intrinsic barrier? Results from the solution reactions shown in eqs 3[18] and 4[19] indicated a *decrease* in the intrinsic barrier with increasing aromaticity
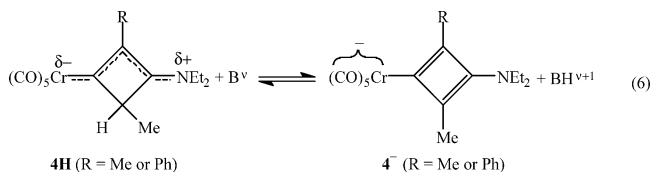
$$C_5H_5(NO)(PPh_3)Re \overset{+}{=}\!\!\!\diagdown\!\!\!\diagup_{X} + B^{\nu} \rightleftharpoons C_5H_5(NO)(PPh_3)Re\!\!\diagdown\!\!\!\diagup_{X} + BH^{\nu+1} \quad (3)$$

1H⁺-O (X = O)   **1-O** (X = O)
1H⁺-Se (X = Se)   **1-Se** (X = Se)
1H⁺-S (X = S)   **1-S** (X = S)

$$\quad + B^{\nu} \rightleftharpoons \quad + BH^{\nu+1} \quad (4)$$

2H-O (X = O)   **2⁻-O** (X = O)
2H-S (X = S)   **2⁻-S** (X = S)

of the product, that is, $\Delta G_0^{\ddagger}(O) > \Delta G_0^{\ddagger}(Se) > \Delta G_0^{\ddagger}(S)$ for eq 3[18] and $\Delta G_0^{\ddagger}(O) > \Delta G_0^{\ddagger}(S)$ for eq 4.[19] According to the PNS,[4] these results imply that the development of aromaticity is *ahead of proton transfer* at the transition state. The study of a third reaction, eq 5, yielded $\Delta G_0^{\ddagger}(O) < \Delta G_0^{\ddagger}(S)$.[20] However, a detailed analysis[19,20] revealed that the observed reactivity order is an artifact
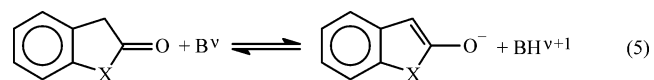
$$\quad =\!\!O + B^{\nu} \rightleftharpoons \quad \!\!-O^{-} + BH^{\nu+1} \quad (5)$$

3H-O (X = O)   **3⁻-O** (X = O)
3H-S (X = S)   **3⁻-S** (X = S)

stemming from other factors that mask the $\Delta G_0^{\ddagger}$-lowering effect of the increased aromaticity of **3⁻**-S.

In addition to eqs 3−5, we have also investigated a system, eq 6, where proton transfer from a Fischer carbene complex leads to the formation of an *anti*aromatic species (**4⁻**).[21] In this

$$(CO)_5\overset{\delta-}{Cr}\!\!=\!\!\diagup\!\!\overset{R}{\diagdown}\!\!\overset{\delta+}{=}\!\!NEt_2 + B^{\nu} \rightleftharpoons (CO)_5Cr\!\!-\!\!\diagup\!\!\overset{R}{\diagdown}\!\!-NEt_2 + BH^{\nu+1} \quad (6)$$

4H (R = Me or Ph)   **4⁻** (R = Me or Ph)

case, no firm conclusions regarding the effect of antiaromaticity on the intrinsic barriers could be reached because too many other factors affect these barriers.

Inasmuch as aromaticity and resonance may be related, the results from the study of reactions 3−5 seem surprising. There is a need to establish the generality of our findings and to corroborate (or refute) them using other methodologies. In the present article, we report a computational study of gas-phase identity carbon-to-carbon proton transfers in two proto-typical aromatic systems and one prototypical antiaromatic system. The specific reactions are shown in eqs 7−9; eqs 7b, 8b, and 9b represent the corresponding noncyclic and nonaro-matic (antiaromatic) analogues, which serve as reference systems.

$$\quad + \quad \rightleftharpoons \quad + \quad \quad (7a)$$

$$\quad + \quad \rightleftharpoons \quad + \quad \quad (7b)$$

$$\quad + \quad \rightleftharpoons \quad + \quad \quad (8a)$$

$$\quad + \quad \rightleftharpoons \quad + \quad \quad (8b)$$

$$\quad + \quad \rightleftharpoons \quad + \quad \quad (9a)$$

$$\quad + \quad \rightleftharpoons \quad + \quad \quad (9b)$$

Our approach involves not only the calculation of possible energetic effects on the intrinsic barriers of reactions 7−9 but also of other indices that may serve as measures of aromaticity such as geometric parameters, HOMA,[22,23] and NICS[24,25] values. This is important in putting any emerging conclusions on firmer ground because aromaticity is not a directly measurable or

(10) Computational results in the gas phase have generally confirmed the presence of transition-state imbalances in these reactions[11−16] although other factors such as field and polarizability effects often offset the π-acceptor effect on the intrinsic barriers.[13c,d]
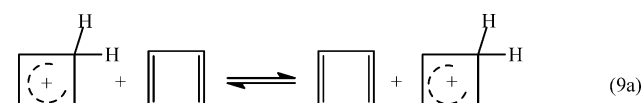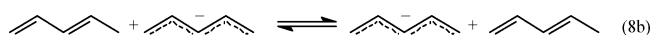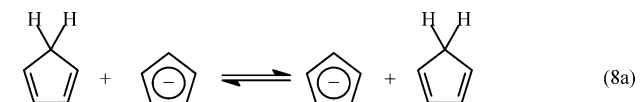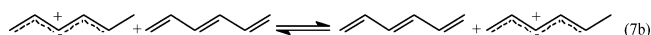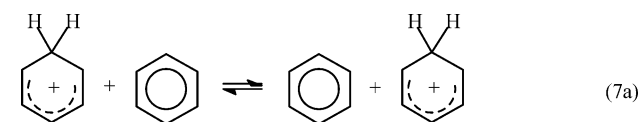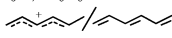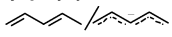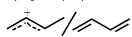
(11) Bekšic, D.; Bertrán, J.; Lluck, J. M.; Hynes, J. T. *J. Phys. Chem. A* **1998**, *102*, 3977.
(12) (a) Saunders, W. H., Jr. *J. Am. Chem. Soc.* **1994**, *116*, 5400. (b) Saunders, W. H., Jr.; Van Verth, J. E. *J. Org. Chem. Soc.* **1994**, *60*, 3452. (c) Van Verth, J. E.; Saunders, W. H., Jr. *J. Org. Chem.* **1997**, *62*, 5743. (d) Van Verth, J. E.; Saunders, W. H., Jr. *Can. J. Chem.* **1999**, *77*, 810. (e) Harris, N.; Wei, W.; Saunders, W. H., Jr.; Shaik, S. S. *J. Phys. Org. Chem.* **1999**, *12*, 259. (f) Harris, N.; Wei, W.; Saunders, W. H., Jr.; Shaik, S. *J. Am. Chem. Soc.* **2000**, *112*, 6754.

Chart 1

TS(C₆H₇⁺/C₆H₆)

(C₆H₇⁺)

TS(C₅H₆/C₅H₅⁻)

C₅H₆

TS(C₄H₅⁺/C₄H₄)

C₄H₅⁺
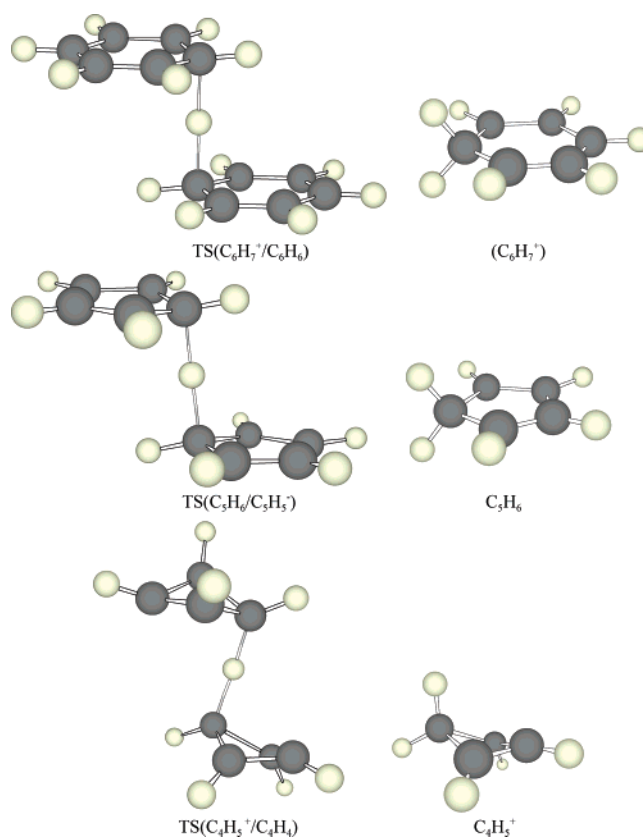
Table 1. Selected Geometric Parameters (MP2/6-311+G(d,p))

System	C---H---C ^{a}	$\alpha_{Reactant}$ ^{c}	α_{TS} ^{c}	$\Delta\alpha$ ^{d}
$C_6H_7^+ / C_6H_6$	1.440 (1.109) ^{b}	50.1	14.5	35.6
$\sim\!\!\sim\!\!\sim\!\!/\!\sim\!\!\sim$	1.445	57.5	25.4	32.1
$C_5H_6 / C_5H_5^-$	1.406 (1.099) ^{b}	53.5	21.9	31.6
$\sim\!\!\sim\!\!/\!\sim\!\!\sim$	1.402	53.0	37.9	15.1
$C_4H_5^+ / C_4H_4$	1.354 (1.088) ^{b}	60.5	52.2	8.3
$\sim\!\!\sim\!\!/\!\sim\!\!\sim$	1.430	57.6	19.8	37.8

^{a} C−H bond at transition state in Angstroms. ^{b} C−H bond in reactant in Angstroms. ^{c} Pyramidal angle (for a definition, see the section on aromaticity indices). ^{d} $\Delta\alpha = \alpha_{reactant} - \alpha_{TS}$ (note that $\alpha_{product} = 0$ in all cases).

uniquely defined property[25] but should be regarded as being "statistically multidimensional."[26]

Results and Discussion

Geometries. The structures that are of particular interest, which include the transition states of reactions 7a, 8a, and 9a, as well as the benzenium ion and the cyclobutenyl cation are

(13) (a) Bernasconi, C. F.; Wenzel, P. J. *J. Am. Chem. Soc.* **1994**, *116*, 5405. (b) Bernasconi, C. F.; Wenzel, P. J. *J. Am. Chem. Soc.* **1996**, *118*, 10494. (c) Bernasconi, C. F.; Wenzel, P. J.; Keeffe, J. R.; Gronert, S. *J. Am. Chem. Soc.* **1997**, *119*, 4008. (d) Bernasconi, C. F.; Wenzel, P. J. *J. Org. Chem.* **2001**, *66*, 968. (e) Bernasconi, C. F.; Wenzel, P. J. *J. Am. Chem. Soc.* **2001**, *123*, 7146. (f) Bernasconi, C. F.; Wenzel, P. J. *J. Org. Chem.* **2003**, *68*, 6870.
(14) Yamataka, H.; Mustanir Mishima, M. *J. Am. Chem. Soc.* **1999**, *121*, 10233.
(15) Lee, I.; Kim, C. K. *J. Phys. Org. Chem.* **1999**, *12*, 255.
(16) Costentin, C.; Savéant, J.-M. *J. Am. Chem. Soc.* **2004**, *126*, 1478.

shown in Chart 1. 3D representations of all of the calculated structures are reported in Figures S1−S36, whereas *schematic* structures that show relevant bond lengths and angles are summarized in Figures S49−S51 (Supporting Information).[27] Some of these geometric parameters are summarized in Table 1. Furthermore, schematic structures that highlight bond lengths for all of the species participating in reactions 7a, 8a, and 9a are shown in Figure 1. We offer the following comments:

(1) For all of the proton transfers, the two fragments of the transition state are in an anti relationship and the C−H−C angle is 180°, except for the $C_4H_5^+/C_4H_4$ system where this angle is 169°. Our findings are in agreement with results for identity proton transfers of the type $Y-CH_3 + CH_2=Y^- \rightleftarrows {}^-Y=CH_2 + CH_3-Y$[12,13] and other similar proton transfers,[28] but contrasts with hydride ion transfers where the two halves are often in a syn relationship and the C−H−C angle is significantly less than 180°.[29−31] We do not attach much significance to the slightly smaller C−H−C angle for the $C_4H_5^+/C_4H_4$ system; enforcing a 180° angle raises the transition-state energy only by 0.5 kcal/mol, and the transition state calculated by the B3LYP method has a 179° angle.

(2) The C−H bond length between the reactive carbon and the proton-in-flight at the transition state varies between 1.35 and 1.45 Å. These variations may be rationalized as follows.

(17) As corollary, a reactant stabilizing factor that is lost ahead of bond changes increases the intrinsic barrier, whereas a reactant stabilizing factor that it lost late reduces the intrinsic barrier. For product and reactant destabilizing factors, the opposite relationships hold.
(18) Bernasconi, C. F.; Ragains, M. L.; Bhattacharya, S. *J. Am. Chem. Soc.* **2003**, *125*, 12328.
(19) Bernasconi, C. F.; Pérez-Lorenzo, M. *J. Am. Chem. Soc.* **2007**, *129*, 2704.

Chart 2
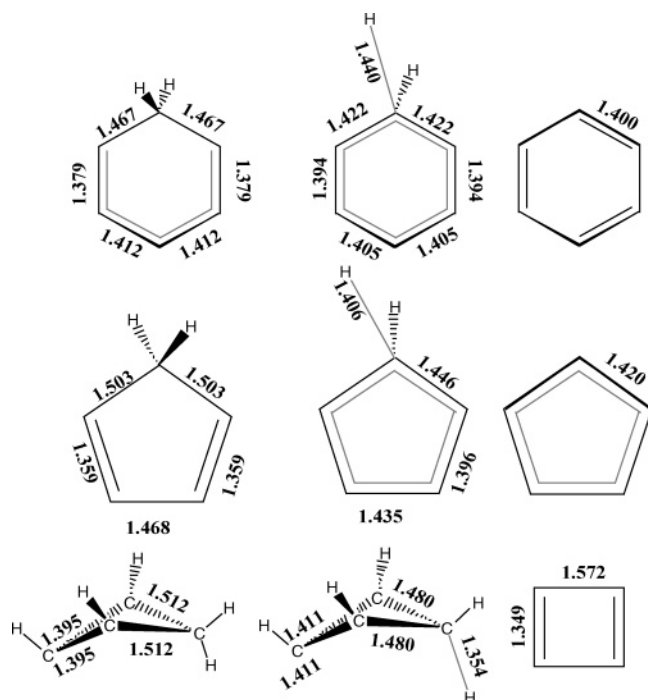
Figure 1. MP2/6-311+G(d,p) bond lengths of species participating in reactions 7a, 8a, and 9a.
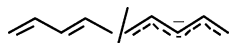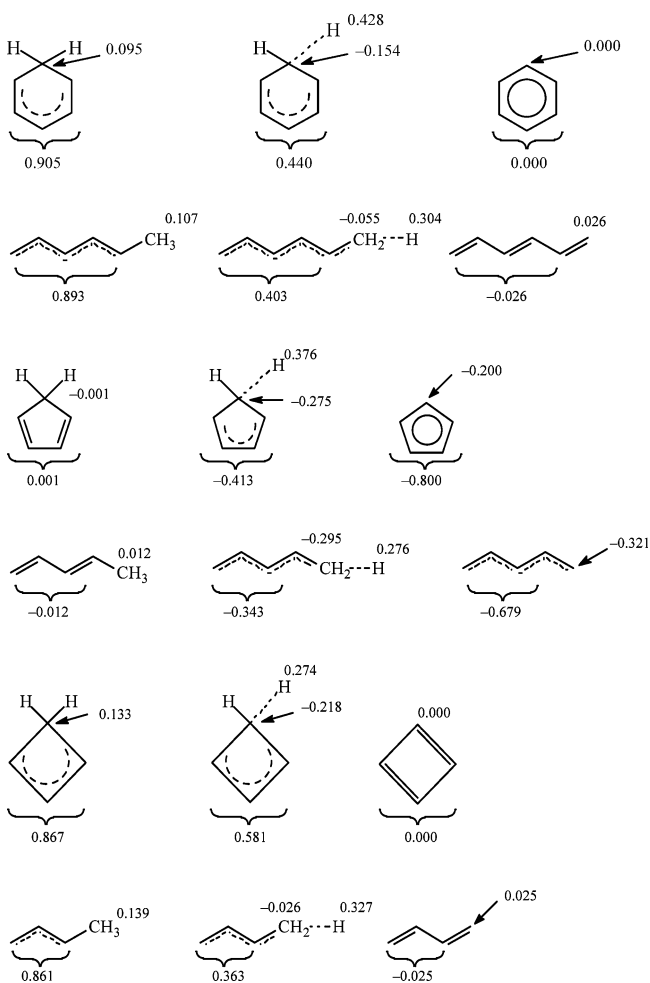
For the

and

systems, these bond lengths are very similar (1.445 and 1.430 Å, respectively) but longer than for the

system (1.402 Å). The tighter bonds for the latter system probably reflect the electrostatic attraction between the positively charged proton-in-flight (Chart 2 below) and the two negatively charged halves of the transition state; this contrasts with the

electrostatic *repulsion* between the proton-in-flight and the two positively charged halves of the transition state for the other two systems, which leads to longer C–H bonds. The same forces operate on the cyclic systems as reflected in the shorter transition-state C–H bond for the $C_5H_6/C_5H_5^-$ (1.406 Å) compared to the $C_6H_7^+/C_6H_6$ system (1.440 Å). However, for the $C_4H_5^+/C_4H_4$ system the C–H bond (1.354 Å) is unusually short. This may be due, at least in part, to the higher s character of the carbon in the smaller ring, which leads to a stronger C–H bond. This is a well-known phenomenon in cyclopropanes;[32] because the CCC angle at the transition state (a in Figure S51[27]) of 69° is almost as small as for cyclopropane, a similarly enhanced s character is expected.[33]

(3) Our structure of the benzenium ion, which is planar and has C_{2v} symmetry is virtually identical to that calculated by Glukhovtsev et al.[34] at the MP2(full)/6-31G(d,p). For the

(20) Bernasconi, C. F.; Zheng, H. *J. Org. Chem.* **2006**, *71*, 8203.
(21) Bernasconi, C. F.; Ruddat, V.; Wenzel, P. J.; Fischer, H. *J. Org. Chem.* **2004**, *69*, 5232.
(22) Krygowski, T. M.; Cyránski, M. K. *Chem. Rev.* **2001**, *101*, 1385.
(23) (a) Kruszewski, J.; Krygowski, T. W. *Tetrahedron Lett.* **1972**, *13*, 3839. (b) Kruszewski, J.; Krygowski, T. M. *Can. J. Chem.* **1975**, *53*, 945. (c) Krygowski, T. M.; Cyrañski, M. K. *Tetrahedron*, **1996**, *118*, 6317.
(24) Schleyer, P. v. R.; Maerker, C.; Dransfeld, A.; Jiao, H.; van Eikema Hommes, W. J. R. *J. Am. Chem. Soc.* **1996**, *118*, 6317.
(25) Chen, Z.; Wannese, C. S.; Corminboeuf, C.; Puchta, R.; Schleyer, P. v. R. *Chem. Rev.* **2005**, *105*, 3842.
(26) Cyranski, M. K.; Krygowski, T. M.; Katritzky, A. R.; Schleyer, P. v. R. *J. Org. Chem.* **2002**, *67*, 1333.
(27) See the paragraph concerning the Supporting Information at the end of this article.
(28) Keeffe, J. R.; Gronert, S.; Colvin, M. E.; Tran, W. L. *J. Am. Chem. Soc.* **2003**, *125*, 11730.
(29) (a) Wu, Y.-D.; Houk, K. N. *J. Am. Chem. Soc.* **1987**, *109*, 906. (b) Wu, Y.-D.; Houk, K. N. *J. Am. Chem. Soc.* **1987**, *109*, 2276.
(30) Gronert, S.; Keeffe, J. R. *J. Am. Chem. Soc.* **2005**, *127*, 2324.
(31) Bernasconi, C. F.; Wenzel, P. J. Unpublished observations.
(32) (a) Yamamoto, S.; Nakata, M.; Fukuyama, T.; Kuchitsu, K. *J. Phys. Chem.* **1985**, *89*, 3298. (b) Rozsondai, B. In *The Chemistry of the Cyclopropyl Group*; Rappoport, Z., Ed.; Wiley & Sons: New York, 1995; Vol. 2, p 139.

(33) The C–H bond of the $C_4H_5^+$ cation (1.088 Å) whose CCC angle (70.7°, Figure S51 in the Supporting Information[27]) is only slightly larger than that of the transition state is also shorter than that of $C_6H_7^+$ (1.109 Å), but here the reduction is not as large as that for the transition state. The unusually short transition-state C–H bond length may be related to the C–H–C angle of less than 180° discussed earlier; the alternative transition state with a 180° angle mentioned above has a C–H bond length of 1.395 Å.
(34) Glukhovtsev, M. N.; Pross, A.; Nicolaides, A.; Radom, L. *J. Chem. Soc., Chem. Commun.* **1995**, 2347.
(35) Sieber, S.; Schleyer, P. v. R.; Otto, H. A.; Gauss, J.; Reichel, F.; Cremer, D. *J. Phys. Org. Chem.* **1993**, *6*, 445.
(36) Maksic', Z. B.; Kovačevic', B.; Lesar, A. *Chem. Phys.* **2000**, *253*, 59.

Table 2. Aromaticity Indices

	α^a	HOMA	NICS(1)
	Eq 7a		
$C_6H_7^+$	50.1	0.415	−6.05
TS	14.5	0.874	−9.26
C_6H_6	0.0	0.963	−10.20
% progress at TS^b	71.0	83.8	77.3
	Eq 8a		
C_5H_6	53.5	−0.791	−5.17
TS	21.9	0.560	−8.33
$C_5H_5^-$	0.0	0.739	−9.36
% progress at TS^b	59.0	88.3	75.4
	Eq 9a		
$C_4H_5^+$	60.5	−0.99	−13.69
TS	52.2	−0.156	−12.64
C_4H_4	0.0	−3.55	18.11
% progress at TS^b	13.7	22.3	3.30

^{a} Pyramidal angle. ^{b} [Index(TS) − Index(Reactant)]/Index(Product) − Index(Reactant)] × 100.

cyclobutenyl cation, we obtained a structure that is very similar to those published by Sieber et al.[35] and Maksic et al.[36] The nonplanarity is a well-known feature driven by homoaromatic stabilization.[37]

(4) As can be seen in Figure 1, for the $C_6H_7^+/C_6H_6$ and $C_5H_6/C_5H_5^-$ systems, there is a smooth equalization of the bond lengths in going from the reactant to the transition state to the product. For example, in $C_6H_7^+$ the C_1-C_2, C_2-C_3, and C_3-C_4 bonds are 1.467, 1.379, and 1.412 Å, respectively, whereas at the transition state they are 1.422, 1.394, and 1.405 Å, respectively, that is, these latter ones approach the situation in benzene where all of the bonds are 1.400 Å. Similarly, in C_5H_6 the C_1-C_2, C_2-C_3, and C_3-C_4 bonds are 1.503, 1.359, and 1.468 Å, respectively, whereas at the transition state they are 1.446, 1.396, and 1.435 Å, respectively, approaching the 1.420 Å bond length in $C_5H_5^-$. Furthermore, the bond lengths at the transition state are much closer to those in the aromatic product than to those in the reactant. This suggests a disproportionately strong development of aromaticity at the transition state.

(5) In contrast to the $C_6H_7^+/C_6H_6$ and $C_5H_6/C_5H_5^-$ systems, there is no smooth transition in the bond lengths from reactants to products in the $C_4H_5^+/C_4H_4$ system: in $C_4H_5^+$ the C_1-C_2 and C_2-C_3 bonds are 1.512 and 1.395 Å, respectively, at the transition state they are 1.480 and 1.411 Å, respectively, whereas for C_4H_4 they are 1.527 and 1.349 Å, respectively (Figure 1). In other words, in this case it is the transition state rather than the product that has the most equalized bonds; the transition state also maintains the symmetry of $C_4H_5^+$, which is different from that of C_4H_4. The most plausible explanation for these findings is that it is energetically more favorable for the transition state to resemble $C_4H_5^+$ than C_4H_4 because it can retain some of the homoaromatic stabilization[38] of the former and avoid much of the antiaromaticity of the latter.

Aromaticity Indices. In Table 2, we report three types of calculated parameters that may serve as approximate mea-

sures of aromaticity or antiaromaticity in the reactants, products, and transition states of reactions 7a, 8a, and 9a. They are,

1. Pyramidal Angle. The pyramidal angle, α, is defined as illustrated for the benzenium ion (**5**) and the transition state (**6**) for reaction 7a (B = benzene). This angle is 0° in the aromatic species.
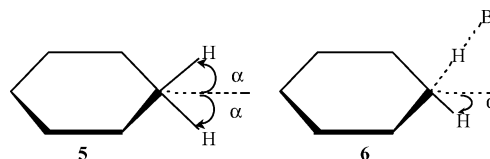
2. Harmonic Oscillator Model of Aromaticity (HOMA). This index is based on treating bonds as harmonic oscillators and calculating stabilization/destabilization energies due to the lengthening/shortening of the C−C bond lengths from their optimal values.[22,33,40]

3. NICS Values. In 1996, Schleyer et al.[24,25] proposed the use of absolute magnetic shieldings computed at the ring centers (nonweighted mean of the heavy atom coordinates) as a new aromaticity/antiaromaticity index called the nuclear-independent chemical shift (NICS). Later, NICS(1) determined 1 Å above the ring center was recognized as being a more reliable measure of aromaticity compared to NICS(0) evaluated at the center,[25] and it is these NICS(1) values that are reported in Table 2.

As can be seen from Table 2, for reactions 7a and 8a involving the $C_6H_7^+/C_6H_6$ and $C_5H_6/C_5H_5^-$ systems, respectively, all of the indices for the transition states are closer to those of the respective aromatic product than to the respective nonaromatic reactant, that is, the percent progress in aromaticity development is >50%.

In contrast, for the $C_4H_5^+/C_4H_4$ system the opposite is true, that is, the percent progress in the development of antiaromaticity at the transition state is much smaller than 50%.[41] These findings are consistent with the conclusions derived from the consideration of how the bond lengths change on going from reactant to product, that is, disproportionately high aromaticity at the transition state of reactions 7a and 8a, and disproportionately low antiaromaticity at the transition state of reaction 9a. The highly negative NICS(1) value for the transition state undoubtedly reflects the homoaromaticity of $C_4H_5^+$,[42] which apparently is strongly preserved at the transition state.

Energies. A. General Considerations. Table 3 summarizes proton affinities ($\Delta H°$) and enthalpic barriers ($\Delta H^\ddagger$) for the three reaction pairs of eqs 7−9 calculated at the MP2/6-311+G(2d) level of theory; a more detailed breakdown into electronic and zero point energies of all species involved is presented in Table S1 of the Supporting Information.[27] Table S1 includes similar calculations at the B3LYP/6-311(2d,p) level. The barriers calculated by this latter method are deemed less reliable due to

(37) The cyclobutenyl cation is known to be homoaromatic.[38,39]
(38) Winstein, S.; Adams, R. *J. Am. Chem. Soc.* **1948**, *70*, 838.
(39) Minkin, V. I.; Glukhotsev, M. N.; Simkin, B. Y. *Aromaticity and Antiaromaticity*; Wiley & Sons: New York, 1994.
(40) For justification, to use HOMA in systems with sp²−sp³-hybridized atoms see Raczynska, E. D.; Kosinska, W.; Osmialowski, B.; Gawinecki, R. *Chem. Rev.* **2005**, *105*, 3561.
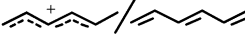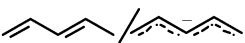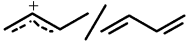
(41) The percentages for a given system are not identical because each index measures a different property and thus cannot be expected to respond to aromaticity or antiaromaticity in exactly the same manner. What is important is that for eqs 7a and 8a the percentages are >50 while for eq 9a they are <50%.
(42) Experimental[43] as well as recent computational estimates[35,36] of the homoaromatic stabilization energy range from 7−9 kcal/mol.
(43) Olah, G. A.; Staral, J. S.; Spear, R. J.; Liang, G. *J. Am. Chem. Soc.* **1975**, *97*, 5489.
(44) Perdew, J. P. *Adv. Quantum Chem.* **1990**, *21*, 113.

Table 3. Proton Affinities, Intrinsic Barriers, and Aromatic Stabilization Energies (MP2//6-311+G(d,p))

System	Reaction	$\Delta H^{\circ a}$	ΔH° (lit.)	$\Delta\Delta H^{\circ b}$	$\Delta H^\ddagger$ (298K)	$\Delta H^\ddagger_{corr}$ (298K)^c	$\Delta\Delta H^\ddagger_{corr}\,^d$	ASE^e
			H$^+$-transfer					
$C_6H_7^+ / C_6H_6$	7a	173.5	179.3^f	−29.2	−12.7	−7.6	−11.1 (−11.8)	−36.3
	7b	202.7	209.7^g		1.0	3.5		
$C_5H_6 / C_5H_5^-$	8a	349.1	353.9^h	−24.9	−2.7	2.2	−7.6 (−8.3)	−29.4
	8b	374.0	362.2^h		6.4	9.8		
$C_4H_5^+ / C_4H_4$	9a	226.6	227.1^i	40.4	0.1	3.6	6.0 (5.3)	38.9
	9b	186.2	187.2^j		−5.6	−2.4		

^{a} ΔH° defined in the direction acid → base + H$^+$. ^{b} $\Delta\Delta H^\circ = \Delta H^\circ$(cyclic) − ΔH°(noncyclic). ^{c} Corrected for BSSE. ^{d} $\Delta\Delta H_{corr}^{\ddagger} = \Delta H_{corr}^{\ddagger}$ (cyclic) − $\Delta H_{corr}^{\ddagger}$ (noncyclic); numbers in parentheses are corrected for steric effects, see text. ^{e} ASE (aromatic stabilization energy) calculated from isodesmic reactions. ^{f} Experimental value: Hunter, E. P.; Lias, S. G. *J. Phys. Chem. Ref. Data* **1998**, *27*, 413. ^{g} Calculated by the CCSD(T)/CBS DFT method: Zhao, Y.; Truhlar, D. G. *J. Phys. Chem. A* **2006**, *110*, 10478. ^{h} Experimental value: Bartmess, J. E. *NIST Standard Reference Data Base*, 19B. NIST negative ion energetics data base, Version 3.00. Standard Reference Data, National Institutes of Standards and Technology, Gaithersburg, MD 20899. ^{i} MP2/6-311+G**// M(II)Calculation, ref 53. ^{j} Experimental value: Lias, S. G.; Ausloos, P. *Int. J. Mass. Spectrom. Ion Processes* **1987**, *81*, 165.

the size-consistency problem in all of the DFT methods.[44] Perdew[44] has shown that in DFT calculations the energy of individual atoms is a function of the number of atoms in a molecule. Because there are twice as many atoms in our transition states compared to either reactants or products, this makes the atoms in the transition states computationally different. Note that the size-consistency problem is a different issue from the basis set superposition error (BSSE), which can be estimated by the counterpoise method (below).[45] No attempt has been made in this work to correct for the size-consistency problem. As in our previous work,[13] we therefore focus our discussion on the MP2/6-311(d,p) results.

Our calculated ΔH° values for the proton affinities are in fair to good agreement with literature values. In the case of benzene, 1,3-butadiene, and cyclopentadiene, the literature values are experimental, whereas for 1,3,5-hexatriene and cyclobutadiene they are computational but at higher levels of theory than ours (references in footnotes of Table 3).

The much lower proton affinity of benzene than that of 1,3,5-hexatriene is mainly due to the aromaticity of benzene, and the same is true for the lower proton affinity of the cyclopentadienyl anion compared to that of the 1,3-pentadienyl anion. This contrasts with the higher proton affinity of cyclobutadiene compared to that of 1,3-butadiene because here the destabilizing effect of antiaromaticity plays a dominant role. There is in fact a good correlation between the differences in proton affinities of the cyclic versus the respective noncyclic reference systems ($\Delta\Delta H^\circ$) and our calculated aromatic stabilization energies (ASE) of the respective aromatic compounds. The $\Delta\Delta H^\circ$ and ASE values are included in Table 3, whereas the correlation, which has a slope of close to unity (0.93), is shown in Figure 2.

The ASEs were calculated on the basis of the isodesmic reactions 10−12; the computational
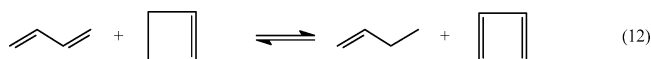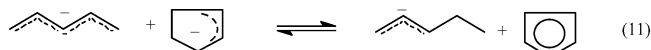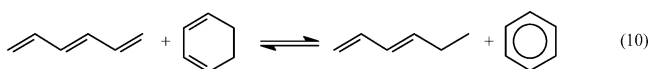
details are reported in Figures S37−S48,[27] and the energy calculations are summarized in Table S1 in the Supporting Information.[27] It should be noted that there is no general agreement as to how to define or determine ASEs, and hence a wide range of such energies have been reported in the literature.[22,39,46] Our approach for calculating these energies is internally consistent; their precise numerical values have no bearing on the qualitative conclusions of this study. Nevertheless, our ASE for benzene (−36.3 kcal/mol) is close to the classic Wheland resonance energy of −36.4 kcal/mol[47] and Wiberg's computational value of −36 kcal/mol,[48] whereas our ASE for the cyclopentadienyl anion (−29.4 kcal/mol) lies somewhere between Bordwell's[49] range of −(24−27) kcal/mol based on acidity data in DMSO, Chestnut and Bartolotti's[50] computational value of −23.3 kcal/mol and the result of a more recent computational approach that yielded −34.5 kcal/mol.[51] Finally, our antiaromatic destabilization energy of cyclobutadiene (38.9 kcal/mol) is close to the computational value of 40.3 kcal/mol of Suresh et al.[52] but greater than a more recent experimental value of 34.2 kcal/mol.[53]

(45) Boys, S. F.; Bernardi, F. *Mol. Phys.* **1970**, *19*, 553.
(46) (a) Schleyer, P. v. R.; Manoharan, M.; Jiao, H.; Stahl, F. *Org. Lett.* **2001**, *3*, 3643. (b) Cyranski, M. K. *Chem. Rev.* **2005**, *105*, 3773.
(47) Wheland, G. W. *Resonance in Organic Chemistry*; Wiley: New York, 1955; (a) p 517, (b) Table 3.7, p 98.
(48) Wiberg, K. B. *J. Org. Chem.* **1997**, *62*, 5720.
(49) Bordwell, F. G.; Drucker, G. E.; Fried, H. E. *J. Org. Chem.* **1981**, *46*, 632.
(50) Chestnut, D. B.; Bartoletti, L. J. *Chem. Phys.* **2000**, *257*, 175.
(51) Wang, L.; Wang, H. J.; Dong, W. B.; Ge, Q. Y.; Lin, L. *Struct. Chem.* **2007**, *18*, 25.
(52) Suresh, C. H.; Koga, N. *J. Org. Chem.* **2002**, *67*, 1965.
(53) Fattahi, A.; Lis, L.; Tian, X.; Kass, S. R. *Angew. Chem., Int. Ed. Engl.* **2006**, *45*, 4984.
(54) (a) Farneth, W. E.; Brauman, J. I. *J. Am. Chem. Soc.* **1976**, *98*, 7891. (b) Moylan, C. R.; Brauman, J. I. *Annu. Rev. Phys. Chem.* **1983**, *34*, 187.
(55) In the cyclic systems, the reaction centers are secondary carbons, whereas in the noncyclic systems they are primary carbons.
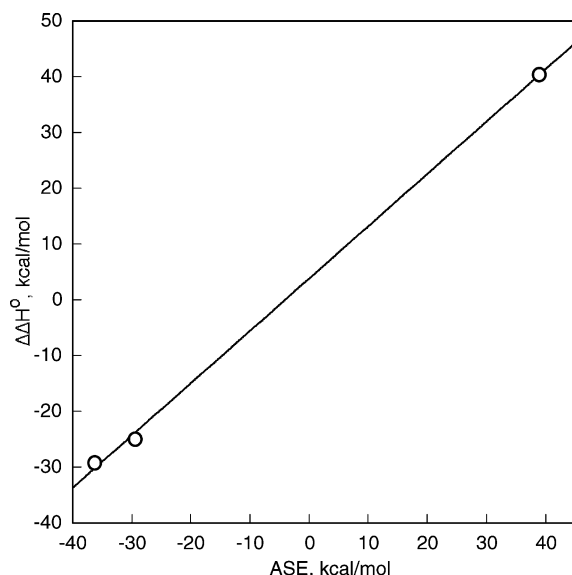
Figure 2. Correlation between $\Delta\Delta H°$ and ASE with $\Delta\Delta H°$ defined in footnote b of Table 3.

The major focus in this article is on the barriers ($\Delta H^{\ddagger}$), which, due to the fact that eqs 7−9 represent identity reactions, are equivalent to *intrinsic* barriers. It should be noted that we use the term barrier for the enthalpy difference between the transition state and the separated reactants and not between the transition state and the ion−dipole complexes, which precede the transition state in gas-phase ion−molecule reactions.[54] This is because those ion−dipole complexes have little relevance with respect to the questions dealt with in this work.

Two sets of $\Delta H^{\ddagger}$ values are reported in Table 3; the first one is uncorrected ($\Delta H^{\ddagger}$), the second is counterpoise corrected ($\Delta H_{corr}^{\ddagger}$) for the BSSE.[45] We shall focus our discussion on the corrected $\Delta H^{\ddagger}$ values. However, because these corrections are quite similar in all cases, none of the qualitative conclusions of this article would change if the uncorrected values were used.

Table 3 includes $\Delta\Delta H_{corr}^{\ddagger}$ values, which refer to the differences between $\Delta H_{corr}^{\ddagger}$ for the cyclic system and $\Delta H_{corr}^{\ddagger}$ for the respective noncyclic reference system. It should be noted that the barriers for the cyclic systems include potential contributions by barrier enhancing steric effects that are larger than those for the respective noncyclic system because of more extensive crowding at the transition state.[55] A conservative estimate of this contribution is on the order of 0.7 kcal/mol.[56] The $\Delta\Delta H_{corr}^{\ddagger}$ values placed inside parentheses (Table 3) take this steric contribution into account.

B. Barriers for the $C_6H_7^+$/C_6H_6 and C_5H_6/$C_5H_5^-$ Systems. The most significant finding is that for the two reactions that involve aromatic systems (eqs 7a and 8a) the barriers are lower than for their respective reference reactions (eqs 7b and 8b, respectively). We also note that the difference between the barrier for the aromatic system and that of the respective noncyclic reference reaction ($\Delta\Delta H_{corr}^{\ddagger}$) is larger for reaction 7a (−11.1 kcal/mol) than for reaction 8a (−7.6 kcal/mol). This

(56) On the basis of rate constant ratios for the deprotonation of $CH_3CH_2NO_2$ versus CH_3NO_2[57] and $(CO)_5Cr=C(OMe)CH_2CH_3$ versus $(CO)_5Cr=C(OMe)$-CH_3[58] by OH^- and piperidine.
(57) Bernasconi, C. F.; Panda, P.; Stronach, M. W. *J. Am. Chem. Soc.* **1995**, *117*, 9206.
(58) Bernasconi, C. F.; Sun, W.; García-Río, L.; Kin-Yan Kittredge, K. *J. Am. Chem. Soc.* **1997**, *119*, 5583.

is consistent with the greater ASE for benzene (−36.3 kcal/mol) than for $C_5H_5^-$ (−29.4 kcal/mol).

Our results imply that the sum of the ASEs of the two halves of the transition state is greater than the ASE of the respective aromatic reactant/product. This is illustrated by the schematic energy profiles shown in Figure 3. The arrows pointing down in parts A and B of Figure 3 represent the aromatic stabilization energies of the reactants (ASE_R), products (ASE_P), and the transition state (ASE_{TS}), respectively. The greater than 50% aromaticity in both halves of the transition state are reflected in the fact that $|ASE_{TS}| > |ASE_R| = |ASE_P|$.

In the terminology of the PNS,[4] the disproportionately high ASE of the transition state is equivalent to the statement that aromatic stabilization develops ahead of proton transfer. In this formulation, $C_6H_7^+$ and C_5H_6 are regarded as the reactants, and C_6H_6 and $C_5H_5^-$ are regarded as the respective products. If the roles of the reactants and products are reversed, one looks at the loss of aromatic stabilization lagging behind proton transfer; either way, the result is a reduced intrinsic barrier. These conclusions are therefore consistent with those reached based on the geometries and aromaticity indices, as well as those derived from the solution-phase reactions 3−5.

C. Barrier in the $C_4H_5^-$ System. Here, $\Delta H^{\ddagger}$ for eq 9a is *higher* than that for the reference reaction 9b ($\Delta\Delta H_{corr}^{\ddagger} = 6.0$ kcal/mol). In keeping with the PNS,[4,17] one possible interpretation of the positive $\Delta\Delta H_{corr}^{\ddagger}$ value would be that antiaromatic destabilization of the transition state develops ahead of proton transfer and hence increases the barrier. However, this is an unsatisfactory interpretation because it is inconsistent with the geometric parameters and aromaticity indices discussed above, both of which indicate a disproportionately *low* level of antiaromaticity at the transition state. In fact, the low level of antiaromaticity indicated by these parameters suggests that, in the absence of other factors, the $\Delta H_{corr}^{\ddagger}$ value should be quite low and probably leading to a negative $\Delta\Delta H_{corr}^{\ddagger}$ value. Hence, the high barrier for this reaction must have a different origin. A plausible source of the increased barrier is angle and torsional strain at the transition state. The situation is schematically represented in part C of Figure 3.

Charges and Charge Imbalances. Group charges for all of the species are summarized in Chart 2; they were derived from NPA atomic charges reported in Figures S52−S54 in the Supporting Information.[27] As has been observed previously,[12,13,28] the proton-in-flight at the transition state carries a significant positive charge, whereas the donor/acceptor site is negatively charged irrespective of whether the proton donor is a cation (eqs 7a, 7b, 9a, 9b) or a neutral molecule (eqs 8a and 8b).[59] This is not surprising because the attractive electrostatic interaction between the proton-in-flight and the negative donor/acceptor sites leads to stabilization of the transition state in either case.

An important question we need to address refers to the potential for charge imbalances at the transition state. In the deprotonation of carbon acids activated by π acceptors, charge delocalization into the π-acceptor always lags behind proton transfer at the transition state or, in the direction of carbanion protonation, localization by its transfer from the π acceptor to
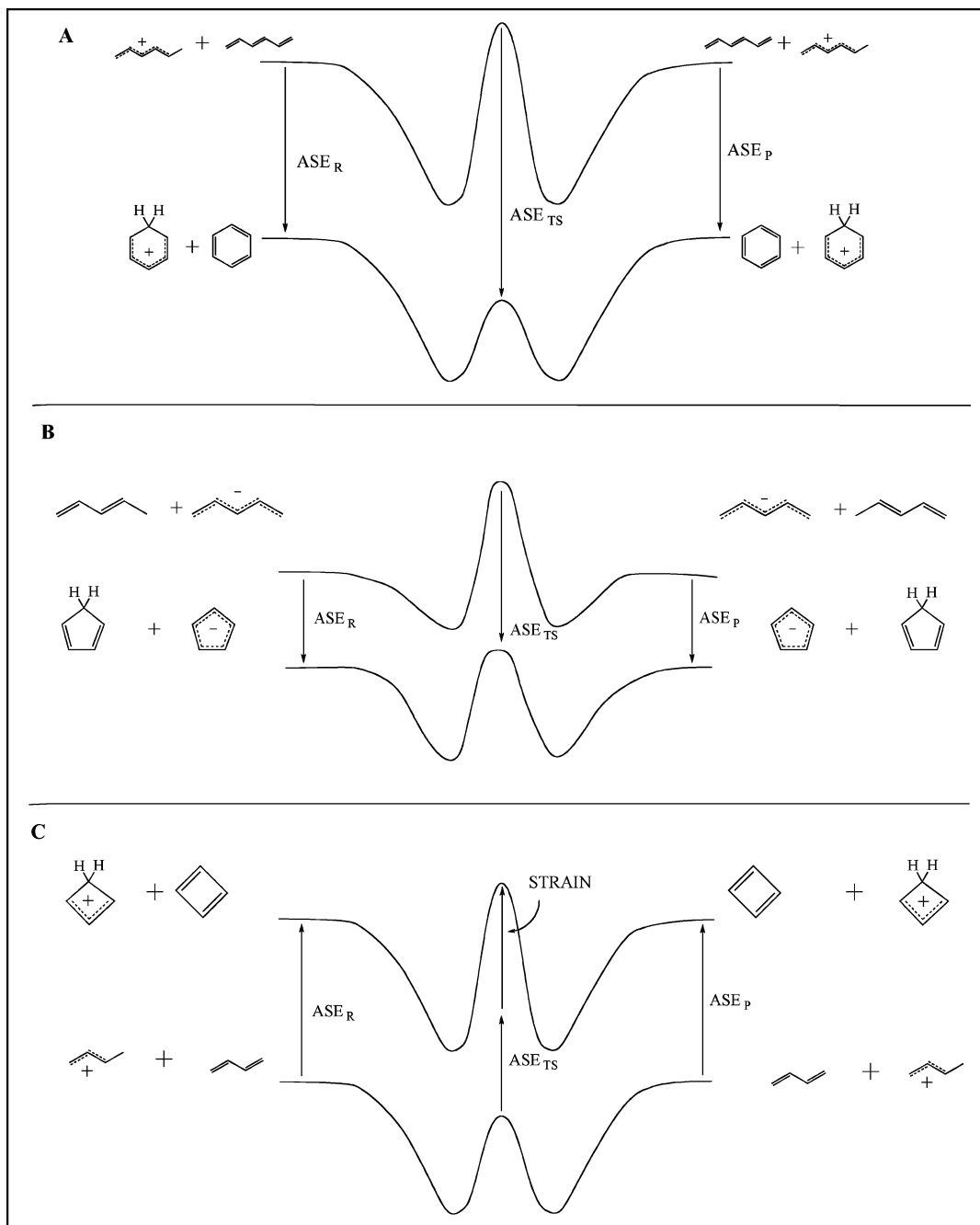
(59) This contrasts with the overall charges on the entire halves of the respective transition states, which, as pointed out above, are positive when the proton donor is cationic but negative when it is a neutral molecule.

Figure 3. Reaction energy profiles for reactions 7a/7b(**A**), 8a,8b(**B**), and 9a/9b(**C**). **A** and **B**: Aromatic stabilization of the transition state is greater than that of benzene or cyclopentadienyl anion, respectively. **C**: Antiaromatic destabilization (positive ASE) of the transition state is less than that of cyclobutadiene; the high barrier results from the additional contribution by angular and torsional strain at the transition state.

the carbon is ahead of protonation. This is schematically shown in eq 2, but the extent of the lag in the delocalization varies with the nature of the π acceptor. Calculations of NPA group charges on reactants/products and transition states of identity reactions such as eq 13 for neutral acid/anionic conjugate base systems,[13a,c,d,f] or eq 14 for cationic acid/neutral conjugate base systems,[13b,13c] allowed a quantitative evaluation of the
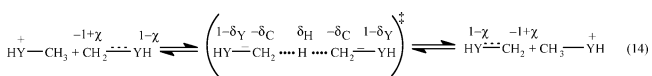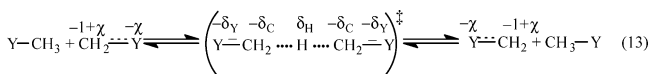
imbalance parameter n defined by eq 15. Equation 15 is the logarithmic form of eq 16, which was derived[13a] by quantifying and

$$n = \frac{\log(\delta_Y/\chi)}{\log(\delta_C + \delta_Y)} \quad (15)$$

$$\delta_Y = \chi(\delta_C + \delta_Y)^n \quad (16)$$

refining Kresge's[9] suggestion that the degree of charge delocalization into Y should be directly related to the degree of C−Y π-bond formation, which in turn depends on the fraction of the charge that has been transferred from the base to the carbon acid.

$$Y-CH_3 + CH_2 \overset{-1+\chi}{=} Y \rightleftharpoons \left(\overset{-\delta_Y}{Y} \overset{-\delta_C}{=} CH_2 \cdots H \cdots \overset{-\delta_C}{CH_2} \overset{-\delta_Y}{=} Y \right)^{\ddagger} \rightleftharpoons \overset{-\chi}{Y} \overset{-1+\chi}{=} CH_2 + CH_3-Y \quad (13)$$

$$\overset{+}{HY}-CH_3 + CH_2 \overset{-1+\chi}{=} \overset{1-\chi}{YH} \rightleftharpoons \left(\overset{1-\delta_Y}{HY} \overset{-\delta_C}{=} CH_2 \cdots H \cdots \overset{-\delta_C}{CH_2} \overset{1-\delta_Y}{=} YH \right)^{\ddagger} \rightleftharpoons \overset{1-\chi}{HY} \overset{-1+\chi}{=} CH_2 + CH_3 \overset{+}{=} YH \quad (14)$$

In a balanced transition state, $n = 1$; for an imbalanced transition state where delocalization lags behind proton transfer, $n > 1$ with n becoming larger with increasing imbalance; for a (hypothetical) situation where delocalization is ahead of proton transfer, $n < 1$. Typical n values for eq 15 or 16 in the gas phase are 1.51, 1.61, 1.52, and 1.59 for Y = CN, CH=CH$_2$, CH=O, and NO$_2$, respectively,[13d] whereas for YH$^+$ = CH=OH$^+$, $n = 1.73$.[13b]

In view of our findings that, for example, for reactions 7a and 8a the development of aromaticity at the transition state is more advanced than proton transfer, an interesting question is whether this would induce charge delocalization to follow the same pattern rather than the usual pattern of delayed delocalization found in nonaromatic systems. Furthermore, what is the situation for the C$_4$H$_5^+$/C$_4$H$_4$ system? In principle, the question may be answered by applying eq 15 to the group charges summarized in Chart 2. However, it needs to be stressed that the situation for reactions 7a, 7b, 9a, and 9b is more complex than that for the reactions of the type of eqs 13 and 14 because there are potentially *two* delocalization processes to consider. We illustrate the problem by first discussing reaction 8a where there is only one delocalization/localization process for which the imbalance is shown schematically and in an exaggerated form in eq 17 (B$^-$ = C$_5$H$_5^-$).

$$B^- + \text{(cyclopentadiene)} \rightleftharpoons \left[\text{(transition state)} \right]^{\ddagger} \rightleftharpoons \text{(cyclopentadienyl anion)} + BH \quad (17)$$
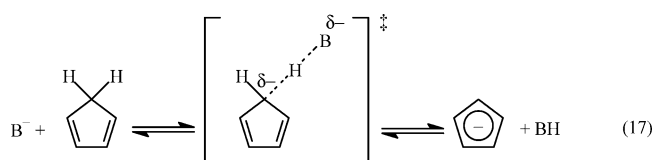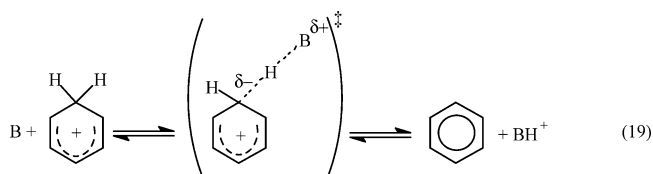
Here, there is no charge on the carbon acid, there is complete charge delocalization in the product, and significant charge localization on the reactive carbon of the transition state (Chart 2). This situation is quite similar to the deprotonation of acetaldehyde, eq 18 (B = CH$_2$=CH−O$^-$), and,

$$B^- + CH_3-CH=O \rightleftharpoons \left(\overset{\delta-}{B}\cdots H\cdots \overset{\delta-}{CH_2}-CH=O \right)^{\ddagger} \rightleftharpoons CH_2=CH-O^- + BH \quad (18)$$
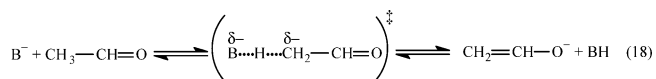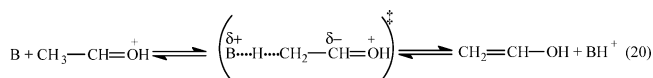
hence, the application of eq 15 to calculate the imbalance parameter n for the C$_5$H$_6$/C$_5$H$_5^-$ system is appropriate. It yields $n = 1.78$,[60] indicating a significant imbalance. Reaction 8b can be treated the same way; one obtains $n = 1.56$, which is about the same as for the CH$_3$CH=O/CH$_2$=CH−O$^-$ system.[13a]

Now consider reaction 7a, shown in more detail in eq 19 (B = benzene). In this case there is also accumulation of negative charge on the reaction center of the transition state (Chart 2), whereas its *delocalization* in the product is tantamount to the neutralization of the positive charge of the benzenium ion. In this regard, the reaction is similar to the carbon deprotonation of oxygen protonated

$$B + \text{(benzenium ion)} \rightleftharpoons \left(\text{(transition state with } \overset{\delta+}{B}\cdots H) \right)^{\ddagger} \rightleftharpoons \text{(benzene)} + BH^+ \quad (19)$$

acetaldehyde, eq 20 (B = CH$_2$=CH−OH). However, what is different is that in the

$$B + CH_3-CH=\overset{+}{OH} \rightleftharpoons \left(\overset{\delta+}{B}\cdots H\cdots \overset{\delta-}{CH_2}-CH=\overset{+}{OH} \right)^{\ddagger} \rightleftharpoons CH_2=CH-OH + BH^+ \quad (20)$$

benzenium ion the positive charge is delocalized but not in CH$_3$CH=OH$^+$. Hence, in reaction 19 there must be an imbalance with respect to this positive charge whose delocalization is expected to lag behind proton transfer in the reverse direction. This problem affects eqs 7a, 7b, 9a, and 9b and renders application of eq 15 problematic. Hence, rather than calculating such n parameters, we simply want to draw attention to the fact that for all proton transfers there is creation and accumulation of negative charge on the reactive carbon of the transition state, which then gets delocalized in the product. This observation indicates that there is imbalance.

Thus, our conclusion is that for all systems, cyclic or noncyclic, aromatic or antiaromatic, charge delocalization lags behind proton transfer. This is an important conclusion; it shows that the development of transition-state aromaticity and charge delocalization are not coupled, a point to which we will return below.

Comparisons with Aromatic Transition States in Other Reactions. Aromaticity in transition states is a well-known phenomenon, especially in pericyclic reactions, as recognized more than half a century ago.[61] A prototypical example is the Diels−Alder reaction of ethylene + 1,3-butadiene → cyclohexene; a computational study by the Schleyer group[62] has shown that the absolute value of the diamagnetic susceptibility, which is a measure of aromaticity, goes through a maximum at the transition state. Similar situations have been reported for other Diels−Alder reactions,[63] for 1,3-dipolar cycloadditions,[64] and enediyne cyclizations,[65] where the aromaticity of reactants, products, and transition states was evaluated using NICS values. A recent report regarding transition-state aromaticity in double group transfer reactions such as the concerted transfer of two hydrogen atoms from ethane to ethylene is also worth mentioning.[66] For many additional examples and references, the review by Chen et al.[25] should be consulted.

It should be noted, though, that in pericyclic reactions aromaticity is mainly a special characteristic of the transition state, whereas the reactants and products are not aromatic or less so than the transition state. Hence, this is quite different

(60) In applying eq 15 to the calculation of n, we use the following definitions: δ_C is the difference between the charge on the reaction center of the transition state (−0.275) and the charge on the same center in the reactant (−0.001) (chart 2); δ_Y is the difference between the charge on the molecular skeleton excluding the reaction center of the transition state (−0.413) and the charge on the skeleton of the reactant proton donor (0.001); χ is the difference between the charge on the molecular skeleton excluding the reaction center of the product (−0.800) and the charge on the same skeleton of the reactant (0.001).

(61) (a) Evans, M. G. *Trans. Faraday Soc.* **1939**, *35*, 824. (b) Dewar, M. J. S. *The Molecular Orbital Theory of Organic Chemistry*; McGraw-Hill: New York, 1969; pp 316−339. (c) Zimmerman, H. *Acc. Chem. Res.* **1971**, *4*, 272.
(62) Herges, R.; Jiao, H.; Schleyer, P. v. R. *Angew. Chem., Int. Ed. Engl.* **1994**, *33*, 1376.
(63) Cossio, F. P.; Morao, I.; Jiao, H.; Schleyer, P. v. R. *J. Am. Chem. Soc.* **1999**, *121*, 6737.
(64) Corminboeuf, C.; Heine, T.; Weber, J. *Org. Lett.* **2003**, *5*, 1127.
(65) Stahl, F.; Moran, D.; Schleyer, P. v. R.; Prall, M.; Schreiner, P. R. *J. Org. Chem.* **2002**, *67*, 1453.
(66) Fernández, I.; Sierra, M. A.; Cossío, F. P. *J. Org. Chem.* **2007**, *72*, 1488.

from the proton-transfer reactions discussed in the present article where the aromaticity of the transition state is directly related to that of the reactants/products. An analogy with steric effects on reaction barriers may illustrate the point. In a reaction of the type of eq 21, steric effects at the transition state will increase the

$$A + B \rightleftharpoons C + D \qquad (21)$$

intrinsic barrier if the reactants are bulky. However, because there are no steric effects on the reactants or products, the concept of early or late development does not apply here, and the same is true for the aromaticity of the Diels–Alder transition state. In contrast, in a reaction of the type of eq 22 there is steric crowding both in the product and the transition state. In this case, the

$$A + B \rightleftharpoons AB \qquad (22)$$

intrinsic barrier will only increase if steric crowding has made disproportionately large progress relative to bond formation at the transition state, but will decrease if development of the steric effect is disproportionately small. This, then, is akin to early or late development of transition-state aromaticity or antiaromaticity in our reactions.

Aromaticity versus Resonance. In reactions that involve resonance-stabilized or delocalized species, there is always an enhanced intrinsic barrier because delocalization invariably lags behind bond changes at the transition state. In view of the fact that nature always chooses the lowest-energy pathway, one wonders why these reactions do not proceed via a transition state with more advanced delocalization, which presumably would be of lower energy. The answer, in the case of proton transfers, is that the delocalization of the negative charge into the π acceptor Y (eqs 2, 13, 14) can *only* occur if there is some development of the C–Y π bond. Hence, the fraction of charge on Y depends on the fraction of π-bond formation, but the fraction of π-bond formation in turn depends on the fraction of charge transferred from the base to the carbon acid.[9] This imposes an insurmountable constraint on the transition state because the charge on Y can never be very high because it represents only a fraction of a fraction. This also means that *n* in eqs 15 and 16 is always >1. Similar arguments apply to other reactions involving resonance-stabilized reactants or products.[4b,4c]

For the reactions that involve the formation of aromatic products such as those studied in the present article as well as reactions 3–5, no such constraints seem to apply to the development of aromaticity. This means that they can take advantage of the extra stabilization of the transition state that derives from strongly developed aromaticity and leads to lower intrinsic barriers. The fact that theses transition states are so highly aromatic suggests that only relatively minor progress in the creation of the appropriate orbitals, or the establishment of their optimal alignment and distances from each other (bond

lengths), may be required for aromatic stabilization to become effective. This notion is supported by a diversity of observations. For example, the NICS of Kekulé benzene (r_{CC} fixed at 1.350 and 1.449 Å) is only 0.8 ppm less than the NICS of benzene itself or, with 1.33 Å (ethylene-like) and 1.54 Å (ethane-like), the NICS is only 2.6 ppm less than that of benzene.[24] Similarly, calculated distortion energies of benzene where every other C–C bond length was varied by 0.01 Å increments (from rCC = 1.40 to 1.34) while all other geometric parameters were allowed to adjust, were found to be quite small.[67] Furthermore, the NICS value for **6** (-8.1)[69] is quite close to that of benzene (-9.7)[24]

6
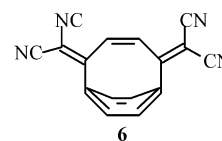
even though there is strong bending of the benzene ring. The same is true for a benzene whose geometry was constrained to that of **6**.[69,70] Comparable results have been reported for highly bent pyrene systems.[71] Also relevant is that the transition state for the trimerization of acetylene to form benzene is highly aromatic based on NICS calculations,[72] despite the fact that the reaction is highly exothermic, which, according to the Hammond postulate,[73] should make the transition state more reactant-like.

An additional factor that probably contributes to an enhancement of the aromaticity of the transition states in the $C_6H_7^+/C_6H_6$ and $C_5H_6/C_5H_5^-$ systems is the fact that the proton-in-flight carries a substantial positive charge. In the $C_6H_7^+/C_6H_6$ system, this reduces the net positive charge in the two C_6H_6 fragments of the transition state to 0.289 per fragment, which is much less than 0.5. This means that these fragments have lost much of the benzenium ion character and have become much more benzene-like. For the $C_5H_6/C_5H_5^-$ system, the positive charge on the proton enhances the negative charge in the two C_5H_6 fragments to -0.688 per fragment, which is substantially more negative than -0.5. Hence, once again the two fragments have become more like the aromatic product than its nonaromatic precursor.

It should perhaps be pointed out that, strictly speaking, there are two main factors that affect the barriers in the aromatic systems: the barrier-lowering effect of aromaticity and the barrier-enhancing effect of incomplete delocalization at the transition state. Apparently, the aromaticity effect is dominant, and hence the net result is a lower barrier.

For the $C_4H_5^+/C_4H_4$ system, no constraints like the ones for resonance-stabilized systems exist either, and hence the reactions can choose a lower-energy pathway by minimizing antiaromaticity of the transition state. Furthermore, the homoaromaticity of $C_4H_5^+$ is substantially retained at the transition state. Hence, both PNS effects, that is, the late loss of a reactant stabilizing factor, homoaromaticity, and the late development of a product destabilizing factor, antiaromaticity, should lower the barrier.

Conclusions

The proton transfers involving the two aromatic systems (eqs 7a and 8a) have substantially lower intrinsic barriers than their

(67) For example, for r_{CC} = 1.38 Å with the alternating r_{CC} = 1.405 Å the distortion energy is 0.55 kcal/mol, and for r_{CC} = 1.36 Å with the alternating r_{CC} = 1.41 Å it is 2.26 kcal/mol.[68]
(68) Keeffe, J. R. Personal communication.
(69) Tsuij, T.; Okuyama, M.; Ohkita, M.; Kawai, H.; Suzuki, T. *J. Am. Chem. Soc.* **2003**, *125*, 951.
(70) For other examples, see ref 25.
(71) Bodwell, G. J.; Bridson, J. N.; Cyrañski, M. K.; Kennedy, J. W. J.; Krygowski, T. M.; Mannion, M. R.; Miller, D. O. *J. Org. Chem.* **2003**, *68*, 2089.
(72) Morao, I.; Cossío, F. P. *J. Org. Chem.* **1999**, *64*, 1868.
(73) Hammond, G. S. *J. Am. Chem. Soc.* **1955**, *77*, 334.
(74) Frisch, M. J. et al. *Gaussian 98*, Revision a.7.

respective noncyclic reference reactions (eqs 7b and 8b, respectively). This is consistent with solution-phase kinetic results for reactions 3−5. According to the PNS, these findings imply a disproportionately strong development of aromaticity in the transition states of these reactions. Aromaticity indices of these transition states, such as NICS(1), HOMA, and others, also indicate a high degree of aromaticity. The high degree of transition-state aromaticity is in stark contrast with the delayed charge delocalization at the transition state, as is apparent qualitatively from the group charges in Chart 2 and quantitatively from the *n* value of 1.78 calculated for the $C_5H_6/C_5H_5^-$ system. This means that reactions involving aromatic systems can reduce their barriers by harnessing the energy-lowering effect of the excess transition-state aromaticity, whereas the constraints imposed on charge delocalization do not allow the lowering of barriers but instead lead to their enhancement.

The reactions involving the antiaromatic cyclobutadiene (eq 9a) have a significantly higher intrinsic barrier than its respective noncyclic reference reaction (eqs 9b). The reason for this is not that the transition state has a disproportionately high degree of antiaromaticity but that angle and torsional strain of the transition state raises the barrier. In the absence of this strain, the barrier for reaction 9a would probably be lower than that for reaction 9b.

The disproportionately high aromaticity of the transition states in the reactions involving aromatic systems suggests that only relatively minor progress in the creation of the appropriate orbitals or their optimal alignment is required for aromatic stabilization to become effective. This is consistent with findings that geometrically distorted aromatic molecules often retain much of their aromaticity. There is probably an additional enhancement of the aromatic character of the transition states because the proton-in-flight carries a positive charge.

Calculations. Calculations were carried out using *Gaussian 98*[74] or *Gaussian 03*[75] on either a SUN X4200 2 x Opteron CPU, 8 GB RAM with 72 Gb disk space, or a Sun Blade 1500 with SPARC process Solaris, 8 GB RAM with 490 Gb disk space.

Reactant and product neutrals and ions were drawn in *Chemdraw* and optimized first with MM2. Inputs for *Gaussian 03* or *Gaussian 98* were then prepared in Cartesian coordinates. Optimization was first done at 3-21G* and was followed by optimization at B3LYP/6-311+G(2d,p) and finally at MP2/6-311+G(d,p). Benzene required further manipulation: a completely planar form of benzene at MP2/6-311+G(d,p) is known to give imaginary modes.[76] Small distortions (4.5° dihedral angles between adjacent C−H bonds) eliminated the imaginary modes.

Transition-state structures required optimization via z-matrix coordinates. Z-matrix construction exploited the proton as the center of symmetric inversion. Proton transition states involving benzene or the cyclopentadienyl anion further exploited the high symmetry of the structures. Bond lengths and angles were assigned to yield a plane of symmetry perpendicular to the plane of the cyclic rings, the symmetry plane passing through the transferred proton. A single improper rotation, S_1, further reduced the number of variables assigned. Thus, C_S symmetry

was exploited for these structures, resulting in a single imaginary vibrational mode.

Transition-state optimization for the $C_4H_5^+/C_4H_4$ system led to a structure in which the carbon fragments maintained the general shape of the homoaromatic cyclobutenyl cation. Optimization at both MP2/6-311+G(d,p) and B3LYP/6-311+G(d,p) levels led to two imaginary modes, one corresponding to the motion of the proton-in-flight (-888 and -1007 cm^{-1}, respectively) and a second corresponding to rotation about the axis of the proton-in-flight (-44 and -18 cm^{-1}, respectively). Allowing free rotation about this axis did not eliminate these latter imaginary modes. The resulting structure seen in Chart 1 does have a slightly bent C−H−C arrangement (169°). The carbon fragments do not overlap as seen in hydride transfer reactions.[30] The bent arrangement and the second imaginary mode are most likely a consequence of the very short distance between the basic carbon and the proton-in-flight.

The transition state for the linear pentadiene system proceeded via z-matrix input with the generation of a single imaginary mode. A second pass of optimization in Cartesian coordinates led to no change in geometry or energy. Thus, the z-matrix input appeared to have no internal constraints. The carbon fragments were free to rotate about the axis of the proton-in-flight, and their negative charges resulted in an anti configuration. The proton travels in a completely straight line connecting the two basic carbon atoms.

For the transition states of the linear butadiene and hexatriene systems, the optimization proceeded at B3LYP/6-311+G(2d,p) to yield a single imaginary mode. However, at MP2/6-311+G-(d,p) optimization without constraint resulted in structures lacking imaginary modes. Constraining the distance between the proton-in-flight and the nearest carbon atom allowed a systematic study of energy versus this length. The length was varied until an imaginary mode was determined (less than -400 cm^{-1} was the criterion). Thus, the results obtained here are 1.5 to 3.0 kcal/mol greater than the lowest-energy optimized MP2/6-311+G(d,p), with the optimization lacking an imaginary mode.

All of the MP2 calculations were carried out using the frozen-core methods, the default for *Gaussian 03*. NMR (NICS1) calculations are reported using the default, using the full correlation, and only the frozen-core energies are reported. All of the vibrational modes were scaled[77] to obtain the zero-point energy and a thermal correction through the partition function of the vibrations. In all cases, a BSSE was calculated by the counterpoise method[45] and reported.

Supporting Information Available: Figures S1−S48 (results of calculations), Table S1 (energies), and refs 74 and 75. This material is available free of charge via the Internet at http://pubs.acs.org.

JA078185Y

(75) Frisch, M. J. et al. *Gaussian 03*, Revision D.01.
(76) Vladimiroff, T. *THEOCHEM* **2000**, *507*, 111.

(77) Scott, A.; Radom, L. *J. Phys. Chem.* **1996**, *100*, 16502.